5016 *Chem. Mater.* **2009,** *21,* 5016–5021
DOI:10.1021/cm901205q

CHEMISTRY OF MATERIALS
Article

Selective Water Uptake in Calcium Oxalate Monohydrate Kidney Stones

Usama Al-Atar,[†] Andrew R. Lewis,[†] Joel M. H. Teichman,[‡] Ben H. Chew,[‡] Byron D. Gates,[†] and Neil R. Branda*,[†]

[†]*4D LABS, Department of Chemistry, Simon Fraser University, Burnaby, British Columbia, Canada, and* [‡]*Department of Urologic Sciences, University of British Columbia, Vancouver, British Columbia, Canada*

Received April 30, 2009. Revised Manuscript Received August 31, 2009

Here we report the amount and location of fluid water absorbed by calcium oxalate monohydrate (COM) kidney stones evaluated using controlled humidity and magnetic resonance imaging (MRI). COM stones subjected to rehydration in a controlled humidity chamber for 16 h at 37 °C absorb approximately 3 wt % water, most of which resides only in thin outer shells of the stones and not within their cores. Although scanning electron microscopy (SEM) shows that there are differences in texture between the inner surface of the water-absorbing shell and the outer surface of the nonabsorbing core, energy-dispersive X-ray (EDX) spectroscopy does not reveal any differences in elemental composition between the two surfaces, and X-ray diffraction (XRD) of powered samples shows them to be similar in crystalline nature. The fact that COM stones do not absorb a significant amount of fluid water beyond their thin outer coatings, which have a different (albeit unidentified) interfacial material separating them from the bulk of the stones, may be the reason for the differences in sensitivity to common medical treatment options such as shock wave lithotripsy.

1. Introduction

The development of new man-made materials has significantly advanced numerous applications ranging from alternative energy and information technologies to biotechnology. The identification of unknown or new classes of naturally occurring materials has equal importance, especially in health sciences, and is the focus of the studies reported in this paper. Although calcium oxalate is a well-known chemical, its materials properties in its naturally occurring form are still under investigation given that it is the culprit in the growth of one of the most common biomineral problems, kidney stones. Because urinary stone disease affects approximately 10% of the U.S. population,[1] causes extreme discomfort, and often leads to renal deterioration (occurring in up to 28% of staghorn renal calculi),[2] probing the makeup of kidney stones in ways that have not been reported will provide useful information to clinicians and urologists. A better understanding of their materials properties may help prevent stones from forming in the first place or offer insights into how best to treat them after they have formed.

Calcium oxalate monohydrate (COM) kidney stones are the most common type[3] making COM one of the most critical biomaterials to fully characterize. Another reason is that the response of COM stones to shock wave lithotripsy (SWL), the most frequently used surgical treatment, is variable[4−6] and patients often require several SWL treatments, which increases the likelihood of adverse effects.[7] An additional concern is that any stone fragment remaining in the kidney after SWL may act as a nidus (a central point of origin) for the growth of further stones.[8,9] Because SWL induces fragmentation through cavitation, where water on the stone absorbs SWL energy to induce vapor bubbles that collapse, rupturing the mesoscopic structure,[10] the inconsistency of SWL to fragment COM stones may be due to the arrangement of the calcium oxalate monohydrate crystals that constitute the stone and how the structure localizes absorbed fluid. Therefore, a deeper understanding of the water-absorbing behavior of COM kidney stones and where absorbed fluid water is found within the stones' structures may offer insights into how to improve noninvasive means to treat stone patients. For example, if water penetrates a stone, it implies porosity and ability to target the inside of the stone with SWL. It also implies the ability (theoretically) to deliver sensitizing agents to enhance SWL efficacy.

Our interests in understanding the materials properties of kidney stones prompted us to probe deeper into their

*To whom correspondence should be addressed. Phone: (778) 782-8061. Fax: (778) 782-3765. E-mail: nbranda@sfu.ca.

(1) Teichman, J. H. *New Engl. J. Med.* **2004**, *350*, 684–693.
(2) Teichman, J. H.; Long, R. D.; Hulbert, J. C. *J. Urol.* **1995**, *153*, 1403–1407.
(3) Brien, G.; Schubert, G.; Bick, C. *Eur. Urol.* **1982**, *8*, 251–256.
(4) Williams, J. C. Jr; Saw, K. C.; Paterson, R. F.; Hatt, E. K.; McAteer, J. A.; Lingeman, J. E. *Urology* **2003**, *61*, 1092–1096.
(5) Teichman, J. M. H.; Portis, A. J.; Cecconi, P. P.; Bub, W. L.; Endicott, R. C.; Denes, B.; Pearle, M. S.; Clayman, R. V. *J. Urol.* **2000**, *164*, 1259–1264.
(6) Zhong, P.; Preminger, G. M. *J. Endourol.* **1994**, *8*, 263–268.
(7) McAteer, J. A.; Evan, A. P. *Semin. Nephrol.* **2008**, *28*, 200–213.
(8) Bellman, G. C. *J. Urol.* **1997**, *158*, 356.
(9) Saw, N. K.; Rao, P. N.; Kavanagh, J. P. *Urol. Res.* **2008**, *36*, 11–15.
(10) Kang, H. W.; Lee, H.; Teichman, J. H.; Oh, J.; Kim, J.; Welch, A. J. *Lasers Surg. Med.* **2006**, *38*, 762–772.

 Published on Web 10/08/2009

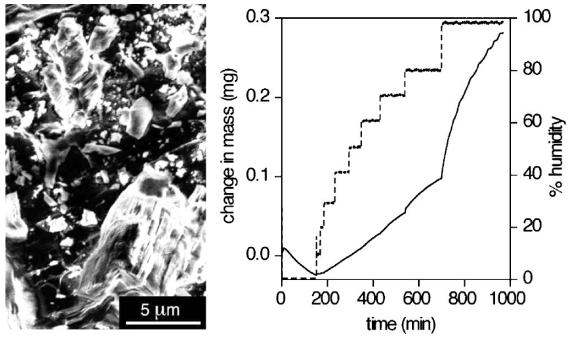

Figure 1. (Left) SEM image of the surface of a piece of COM stone cut with razor blade. (Right) Change in mass of a piece of COM kidney stone (solid line) as the percent humidity within a controlled humidity chamber is increased (broken line).

meso- and microscopic structures. The lack of homogeneity, which may influence water porosity and susceptibility to SWL-induced fragmentation, is clearly observed from scanning electron microscopy (SEM) images of COM kidney stones taken by us (see Figure 1) and others.[11,12] An appreciation of the rough and uneven landscape immediately apparent in these images suggests that water should be able to freely flow through voids within the COM structure. A prior study of stone morphology showed that COM crystals are laminated and polygonal, but with some amorphous regions, which implies structural heterogeneity.[13] Whether water can penetrate uniformly throughout the stone is less apparent and is the subject of our study. Here we demonstrate that COM stones do not absorb a significant amount of liquid water beyond the outer coating, which has a different (albeit unidentified) interfacial material separating it from the bulk of the stone's core. These claims are based on investigations using controlled humidity, magnetic resonance imaging (MRI), electron microscopy, and X-ray diffractometry. As will be argued in this paper, the observed water-localizing phenomenon is not a result of the surface effects of the different materials nor is it due to a change in the material itself, but rather appears to be an intrinsic property of the COM stone structure.

2. Experimental Procedures

Materials. A total of 10 calcium oxalate monohydrate (COM) stones were analyzed (only those used in MRI are shown in Figure 2). They were obtained from percutaneous nephrolithotomy procedures and were identified first using infrared spectroscopy and then using X-ray diffraction (XRD) by comparing the results to those obtained by analyzing commercially available (Fisher Scientific) calcium oxalate monohydrate crystals. The stones were obtained only 3 months prior to the experiment and dried immediately following percutaneous stone removal. Stone sizes ranged from 0.5 to 1 cm. Both whole and fragmented stones were analyzed.

Analysis of Water Uptake Using Controlled Humidity. Fragments from two COM stones were cut from whole stones using a razor blade. The pieces from the two stones were weighed to be 11.5159 and 41.6254 mg, respectively. Each piece was individually placed in a humidity chamber (Dynamic Vapor Sorption, Surface Measurement Systems Ltd., UK) at 37 °C, and dry nitrogen was flushed through the chamber for an appropriate period of time (approximately 150 min for the sample analyzed in this study) until the weight of the fragment had equilibrated. After equilibration, the humidity in the chamber was increased to 95% in 10% increments, with a delay programmed between each increment until the weight of the stone stabilized to within 2×10^{-4} g. The instrument was programmed so that as soon as the sample attained a constant mass (within 0.0002 g) it increased the humidity for the next measurement. The time for this process to occur was very short and accounts for the lack of steplike features in the solid line in Figure 1.

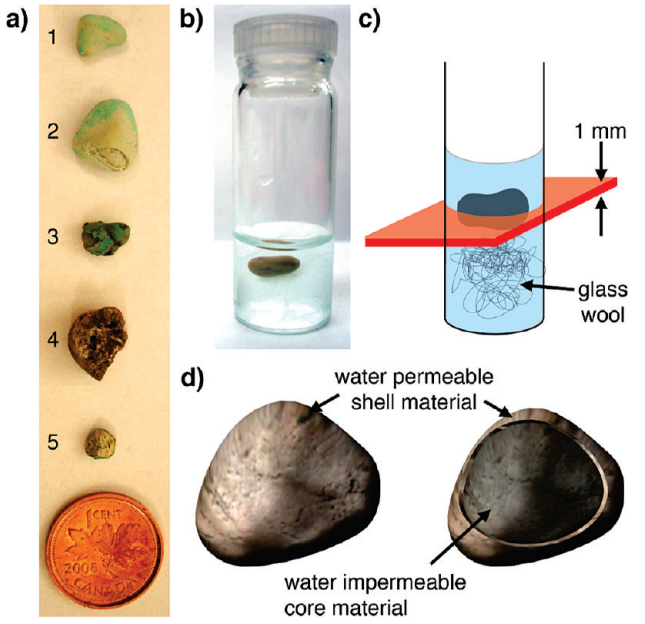

Figure 2. (a) COM kidney stones used for MRI studies. (b) Typical sample preparation of kidney stones showing stone 1 resting on glass wool fibers in a vial containing an aqueous solution (0.01 M) of $CuSO_4$. (c) Cartoon showing orientation of the 1 mm thick horizontal slice of the stone that was imaged. (d) Artistic rendering illustrating our model for a typical COM stone highlighting the shell and core. Stones 1 and 2 were intact during the imaging experiments and the piece that appears missing in the image of stone 2 was removed after these experiments. See text for further details.

Analysis of Water Uptake Using Magnetic Resonance Imaging. MRI studies were conducted on the stones shown in Figure 2 using a Bruker Avance DRX360 NMR spectrometer equipped with microscopic imaging capabilities. The water signal was set at resonance (ca. 360.5 MHz) at 37 °C to acquire the ^1H images. Stones were placed on a small amount of loosely packed glass wool in glass vials containing 0.01 M aqueous $CuSO_4$ (Figure 2b) and the vials were capped to prevent evaporation. Typically, horizontal slices were imaged in the MRI experiments (Figure 2c), although vertical slices show the same trends as those discussed below. Gradient echo fast imaging (GEFI) was used to determine the optimal position of the three 1-mm thick orthogonal (one horizontal, two vertical) slices selected for the quantitative multiecho (ME) imaging experiments within 10−15 min of wetting the stones. Two millisecond sinc-3 pulses were used for both the excitation and refocusing pulses in the ME experiments. A total of 32 echoes were recorded for each slice with 4 scans averaged, the time between echoes (TE) set at 8.2 ms, and a 2 s recovery time between scans (TR). The field of view was fixed at

(11) Sokol, E.; Nigmatulina, E.; Maksimova, N. *Eur. J. Mineral.* **2005**, *17*, 285–295.
(12) Wesson, J. A.; Ward, M. D. *Elements* **2007**, *3*, 415–421.
(13) Khan, S. R.; Hackett, R. L.; Finlayson, B. *J. Urol.* **1986**, *136*, 1367–1372.

20 mm × 20 mm and a matrix size of 256 × 256 was used, producing image voxel dimensions of 0.078 × 0.078 × 1 mm (voxel volume = 0.006 mm^3). The acquisition time for each image was 34 min and each of the three slices was acquired in series until the total soaking time exceeded 24 h. Images were calculated using only the first echo, summing the signals from all 32 echoes (intensity images), and by fitting the (exponential) decay of the echo train intensities for each pixel to create grayscale T_2 images. Higher resolution ^{1}H NMR images were also acquired for some stones after soaking for seven days at 37 °C. The field of view was unchanged but the matrix size was increased to 512 × 512, producing image voxel dimensions of 0.039 × 0.039 × 1 mm (voxel volume = 0.0015 mm^3). The smaller voxel size resulted in correspondingly lower signal intensities so 20 scans were averaged, which increased the total acquisition time to 340 min per slice.

Scanning Electron Microscopy (SEM) and Energy-Dispersion X-ray (EDX) Spectroscopy. Pieces of COM stones were cut using a razor blade and imaged with an SEM (FEI Strata DB 235) at 10 keV to observe surface morphology. After conducting the MRI experiments, the inner surface of the shell and the outer surface of the core of stones 3 and 5 and a stone not subjected to MRI were separated using a razor blade (or forceps in the case of stone 3) and each piece was analyzed by EDX spectroscopy.

X-ray Diffraction (XRD). The outer shells of five COM stones (stones 1, 2, 3, and 4 and a COM stone not subjected to MRI) were separated from the inner core material using a razor blade, or forceps in the case of stone 3. The thickness of the outer shells of stones 2 and 3 were measured using calipers. X-ray diffraction for each layer of stones 3 and 5 (the inner surface of the shell and the outer surface of the core) as well as for the powdered samples of an entire stone was carried out at room temperature using the reflection mode on a Rigaku RAXIS rapid curved image plate detector with graphite monochromator, utilizing a Cu Kα radiation source, a 0.5 mm collimator and 25 min exposure. The reflected X-ray beam was measured from 5 to 100° at 0.02 steps and 2 s per step. Commercially obtained COM crystals (Fisher Scientific) were mounted on a glass-slide (1 cm × 1 cm) and analyzed on the X-ray instrument under similar conditions. Powdered core and shell material diffraction patterns for stones 1−4 and a stone not subjected to MRI were run on the Bruker D8 Advance X-ray diffractometer utilizing a Cu Kα radiation source, a 0.2 mm collimator, 0.02 step size, and run for 10 h.

3. Results and Discussion

A total of ten COM kidney stones are discussed in this paper (not all ten stones are subjected to all experiments). Some of the stones analyzed were completely intact and no signs of broken areas were seen (see stone 1 in Figure 2, for example). Others contained obvious broken areas or were fragments of whole stones (see stones 2 and 4 in Figure 2, for examples).

Water Uptake. The ability of the stones to absorb water was first evaluated on pieces of two kidney stones using a controlled humidity chamber, which provided the incentive for more rigorous MRI experiments. After a small initial drop in mass due to the evaporation of trace water contained within and/or on the surfaces of the stones as a result of constant nitrogen flow, the weights of the stones stabilized. The magnitudes of increase in mass observed after 100% humidity was reached (from 11.4750 to 11.7810 mg and 41.6254 to 42.4626 mg after 968 min) correlate to ∼3% increase in mass (see Figure 1 for a representative example). Because the major aim of the studies described in this paper is to examine where in COM stones absorbed fluid water is located and not to analytically compare how much water is being absorbed, no further stones were analyzed by this technique.

MRI Studies. Although COM kidney stones absorb a significant amount of water, understanding where the water localizes within the stone is more important. Fluid water localization within COM stones was monitored using MRI techniques[14] on five of the whole and fragmented stone samples (Figure 2), and the same trend was observed for all of them. In these experiments, the addition of copper ions was necessary in order to decrease the T_1 relaxation time of the bulk water, which reduces the delay required between successive scans and permits faster data acquisition. The glass wool was used to support the stones, preventing them from resting on the bottom of the vial allowing water to access all surfaces of the stone equally. Glass wool is particularly useful for this purpose because the fibers contain very little water and are thin enough to be almost unobservable in the MRI images. In some samples, air bubbles were observed on the rough surfaces of the stones or fragments and on the glass wool fibers. These bubbles are a result of the air dissolved in the water and are detected because they introduce localized magnetic susceptibility changes at the water−air interfaces. Small artifacts (black hemispheres) from the radio frequency (r.f.) pulses in the coils were also observed at the periphery of the vial, which was close to the coil. The brightest white pixels appearing at the very outer surface of the stones (see Figure 3d, for example) are ascribed to small air bubbles or water experiencing very fast relaxation caused by the presence of a copper salt deposit that forms on selected areas of the outer surfaces of the stones during course of the soaking. This deposit is seen as blue-green coloration on the stones in Figure 2.

MRI analysis on whole COM stones or fragments of them illustrates that liquid water only penetrates the outer shell of the stone and not into the stone's inner core. Representative grayscale images generated from the first echoes of the multiecho MRI experiments for an intact kidney stone (stone 1) and a fragment cut from a previously intact stone (stone 5) are shown in Figure 3. In these images, the grayscale intensity of each pixel corresponds to the signal intensity from the water protons in the corresponding voxel. White pixels correspond to bulk or "liquid" water, black to either no water (or very low amounts), and lighter gray pixels indicate regions having higher water content than the darker gray pixels. Only mobile or liquid water is detected in these images because strongly absorbed or immobile water molecules have broad NMR signals and low signal intensities. This is why the bound water inherent in the COM structure was not observed. Images calculated from the first echoes

(14) GEFI Method and MSME Method. *Paravision User Manual, Version 2.1*; Bruker Medical GMBH: Etlingen, Germany; p 981 and 983.

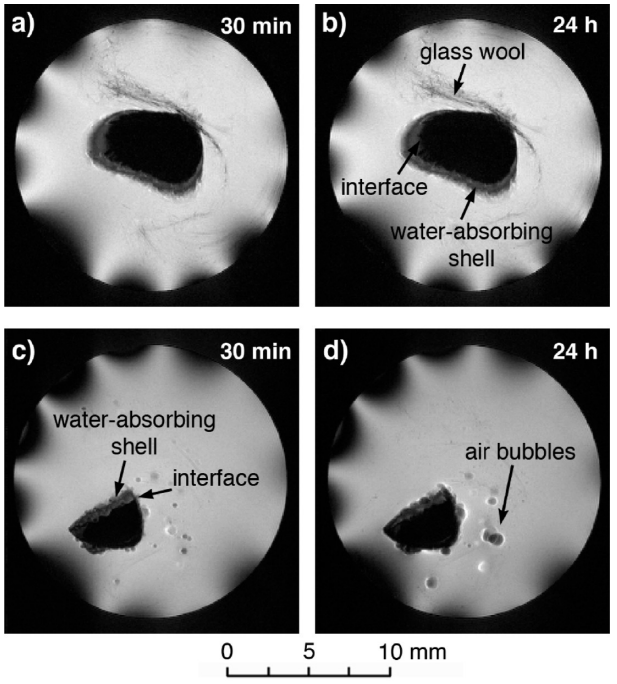

Figure 3. Representative high-resolution ^{1}H NMR images acquired from (a) an intact kidney stone (stone 1) after soaking in an aqueous $CuSO_4$ solution at 37 °C for 30 min, (b) the same stone after soaking for 24 h, (c) a fragment cut from an intact stone (stone 5) after soaking for 30 min, (d) a fragment cut from the same stone after soaking for 24 h. The dark semicircles observed at the periphery of the images are artifacts from the r.f. coil pulses. See text for further details.

provided the most reliable direct detection of water within the stones because the signals have decayed the least due to T_2 relaxation.

The low-resolution, quantitative multiecho (ME) imaging experiments (the gradient echo fast imaging (GEFI) used to locate the stones and determine the optimal position of the three 1 mm thick orthogonal (one horizontal, two vertical) slices for the high-resolution experiments) show that water penetrated the outermost layers of the stones within 10 min, but not the inner stone material. The high-resolution, multiecho images acquired on stone 1 at 37 °C support these initial observations and clearly indicate that significant amounts of water were absorbed only in the outer shell material. A comparison of the first-echo images shows almost no change after soaking for 24 h (images a and b in Figure 3). No liquid water could be detected in the interior material of the stone even after soaking for seven days. Based on the measured image voxel dimensions of 0.078 × 0.078 × 1 mm^3, corresponding to a voxel volume of 0.006 mm^3, and an estimate that water could be detected at less than 20% intensity of full water-containing voxel, the smallest pore detected would have a volume of approximately 0.001 mm^3 (1 nanolitre). Imaging experiments carried out at 22 °C on another intact stone (stone 5 before cutting) showed the same result.[15] Intensity and T_2 images (not shown) confirmed these observations.

It is important to note that although the width of the water-containing outer layer appears thicker on one side

(15) See Supporting Information for details.

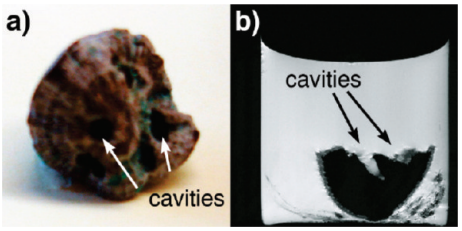

Figure 4. (a) Photograph of stone fragment 4 showing the cavities penetrating through the outer surface of the stone. (b) High resolution ^{1}H NMR image (vertical slice) acquired for the same fragment after 7 days soaking in an aqueous $CuSO_4$ solution at 37 °C clearly showing liquid water in the shell and cavities, but not in the core region. Air bubbles and glass wool are also seen in the image.

of the stone than the other (see Figure 3a, for example), this is not the case as verified by optical measurements. Inconsistencies of this type appear in NMR images whenever the outer shell layer is not completely perpendicular to the imaging plane. They appear because signals from the upper, mid- and lower regions within each 1 mm thick voxel are detected for an angled water-containing layer, which will yield intensity in a number of adjacent pixels, rather than a single pixel in the case where the shell is perpendicular to the imaging plane.

Stone 1 has no visible cracks or breaks in its outer surface (Figure 2a) presumably making it difficult for water to directly travel into spaces between two nonabsorbing surfaces. On the contrary, our MRI observations show that COM stones are composed of a water-absorbing shell surrounding a nonabsorbing core. The fact that the inner material of the stones do not readily uptake water is supported by directly exposing it to water by mechanically fracturing a stone (stone 5) and resubjecting the pieces to the imaging experiments (images c and d in Figure 3). In all cases, water was only detected in the outer shell material even after extended soaking. One of the stone fragments (stone 4) already had a number of indentations that penetrate into the core of the stone as shown in Figure 4, and MRI detected fluid water only within the outer shell and the (now water-filled) cavities. The thickness of the water-absorbing shell of the stones was measured to be 0.3 to 0.5 mm from the high-resolution MRI images and was confirmed by calipers. These data clearly illustrate that the bulk of the material in COM stones is not significantly water-absorbing, and it appears unlikely that the shell and the core material are separated by a barrier impenetrable to water.

SEM and EDX Analysis. SEM images of the inner surfaces of the water-absorbing shells and the outer surfaces of the nonabsorbing cores of two COM stones subjected to MRI analysis (stones 3 and 5) were compared to the two surfaces of a stone not exposed to the $CuSO_4$ solution required for the MRI experiments. The analysis revealed little differences between the treated and untreated stones (images a vs c and b vs d in Figure 5). However, SEM imaging does reveal that the surfaces of the shell and core for either treated or untreated stones have morphological differences. The outer surface of the nonabsorbing core material has larger structural features

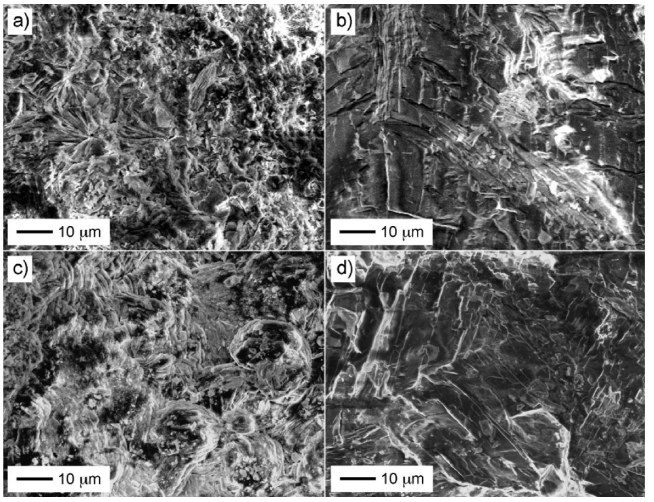

Figure 5. SEM images of (a) the inner surface of the water-absorbing shell, (b) the outer surface of the nonabsorbing core of kidney stone 5, and (c) the inner surface of the water-absorbing shell, (d) the outer surface of the nonabsorbing core of another kidney stone that was not treated with $CuSO_4$.

(image a or c vs image b or d in Figure 5). EDX spectra did not reveal any elemental differences between the materials at the two surfaces.[15]

These types of morphological differences can be expected to result from a preferential growth process. We postulate that stones may go through one growth where COM crystals are added in an orderly and homogeneous fashion, and another growth period where COM crystals are less ordered. It is not likely that these differences are due to any leaching of the Ca^{2+} ions by the Cu^{2+} added as $CuSO_4$ to the water used for the MRI imaging experiments because the morphology of the two surfaces is different even for stones that have not been exposed to $CuSO_4$ (images c and d in Figure 5). There was a small amount of nitrogen observed in both the inner surface of the water-absorbing shell and the outer surface of the nonabsorbing core, which may be due to the presence of proteins, and some reports indicate that protein may play a role in the adhesion and nucleation of COM crystals.[16] Alternatively, the nitrogen peak may also represent the presence of uric acid.

XRD Studies. When the shell and core materials were powdered and analyzed, similar diffraction patterns to crystalline COM were recorded (Figure 6d and 6e). However, when the identities of the crystalline components localized at the surfaces of the two materials (the inner surface of the stone shell and the outer surface of the stone core) were probed, differences between the patterns were observed as shown in patterns a and b in Figure 6. The water-absorbing shell's inner surface has a diffraction pattern similar to that of crystalline COM and also matched that for COM found in the PDF-4 database (International Centre for Diffraction Data reference number 00-013-0601). On the other hand, the XRD pattern for the material localized on the outer surface of

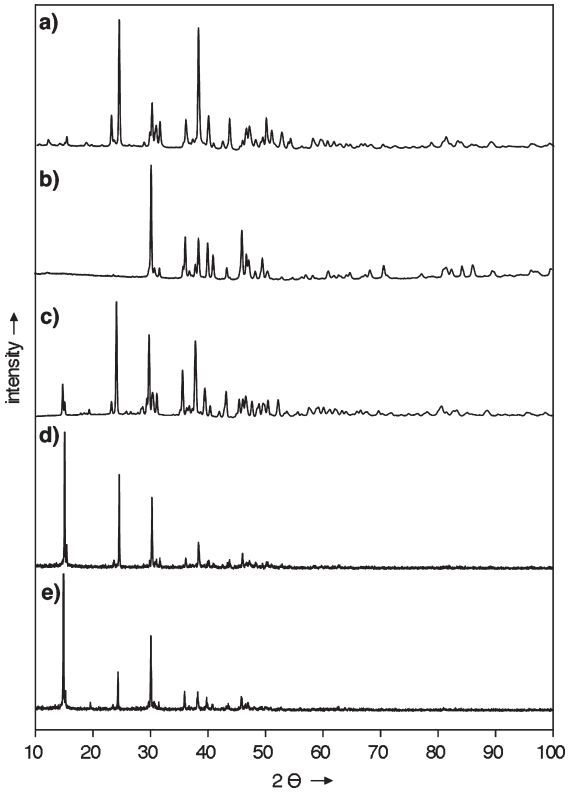

Figure 6. X-ray diffraction pattern of (a) the inner surface of the water-absorbing shell of stone 3, (b) the outer surface of the nonabsorbing core of stone 3, (c) commercially available COM crystals, (d) a powdered sample of the water-absorbing shell material of stone 4, and (e) a powdered sample of the nonabsorbing core material of stone 4. The patterns shown in (d) and (e) are representative of five samples of each stone material.

the nonabsorbing stone core does not match the pattern for COM nor other well-known crystalline materials found in urine. When the shell and core materials were powdered and analyzed, similar diffraction patterns to crystalline COM were recorded (patterns d and e in Figure 6).

The fact that the XRD patterns recorded when a whole COM stone and five samples of core and shell material were powdered and analyzed are similar to the pattern for crystalline COM indicates that the bulk of the calcium oxalate monohydrate material exists in its well-known crystalline form.[13] It also implies that there is a thin layer covering the nonabsorbing core material, as observed by examining our XRD data (Figure 6), but this layer is not responsible for the nonabsorbing nature of the core material, because no fluid water was observed by MRI within the core of a fractured stone stone when it was directly exposed to water (images c and d in Figure 3). The XRD pattern recorded for the nonabsorbing core material does not match that of any components typically found in COM stones such as hydroxyapatite, brushite, uric acid, or calcium oxalate dihydrate. The identity of this crystalline material has yet to be determined. Our data suggest that the bulk of the material is similar in both layers and that water's inability to penetrate the stone's core must be due to an intrinsic property of the core material. We also speculate that the outer nonabsorbing shell may represent crystals most recently added to the

(16) Ryall, R. L.; Fleming, D. E.; Grover, P. K.; Chauvet, M.; Dean, C. J.; Marshall, V. R. *Mol. Urol.* **2000**, *4*, 391–402.

"growing" stone that has yet to fully exclude water if given more time to "mature".

These observations support the growth mechanism where the COM stones grow in layers based on the binding of small crystals to the stone's surface. Growth continues as long as the urine is supersaturated with calcium and oxalate ions. When supersaturation decreases, crystal growth is halted and instead, a fine layer of biomolecules such as proteins, lipids or polysaccharides may coat the stone.[17−19] This deposition could explain the difference in XRD patterns between the inner surface of the water-absorbing shell and the outer surface of the nonabsorbing core. Several studies indicate that proteins such as osteopontin and prothrombin fragment 1 (PTF-1) strongly associate with calcium oxalate crystals.[20,21] When another episode of calcium oxalate supersaturation occurs, this newly formed layer of lipid or protein coating may act as a nidus attracting new COM crystallites to adhere and grow. Altered membrane lipids promote face selective nucleation and retention of calcium oxalate crystals.[22] It may be possible that the water-absorbing shell consists of these newly formed COM crystals (as their identity was confirmed by XRD, Figure 6), whereas the nonabsorbing core is the fully developed crystal aggregate with a protein or lipid coating. Further study is required to determine whether the water-absorbing shell material would eventually convert into the nonabsorbing core material if the COM kidney stone were left longer in the patient.

(17) Dorian, H. H.; Rez, P.; Drach, G. W. *J. Urol.* **1996**, *156*, 1833–1837.
(18) Grases, F.; Costa-Bauza, A.; Conte, A. *Scanning Microsc.* **1993**, *7*, 1067–1073.
(19) Khan, S. R.; Hackett, R. L. *J. Urol.* **1993**, *150*, 239–245.
(20) Ryall, R. L.; Chauvet, M. C.; Grover, P. *BJU Int.* **2005**, *96*, 654–663.
(21) Wesson, J. A.; Ganne, V.; Beshensky, A. M.; Kleinman, J. G. *Urol. Res.* **2005**, *33*, 206–212.
(22) Khan, S. R.; Glenton, P. A.; Backov, R.; Talham, D. R. *Kidney Int.* **2002**, *62*, 2062–2072.

4. Conclusions

To the best of our knowledge, this study is the first instance where the access of water within COM kidney stones has been examined. The findings described in this report indicate that COM kidney stones are composed of a nonabsorbing, water-impermeable core material wrapped with an outer shell that is permeable to water. These results suggest that the inconsistency observed in the treatment of COM stones using SWL theoretically may be due to the inability of water to penetrate deeply into the stone, reducing cavitation bubbles and stone fragmentation. Further investigation into the nature of the porous and nonporous material would enhance the understanding of stone behavior and provide guidelines to develop new noninvasive surgical strategies. Comparison to other stone compositions would also be important and will be the focus of future studies. Our results provide a deeper understanding of the microscopic properties of COM kidney stones, in particular the water-absorbing abilities, and explanations of their variable response to SWL may be considered.

Acknowledgment. This work was supported by the Natural Sciences and Engineering Research Council of Canada (NSERC), the Canada Research Chair Program, and Simon Fraser University (through the SFU Community Trust Endowment Fund). We thank Dr. Colin Fyfe (University of British Columbia) for the use of his MRI instrument.

Supporting Information Available: EDX data of the water-absorbing shells and nonabsorbing cores of a stone subjected to MRI analysis and one not subjected to MRI analysis; MRI image of stone 5 before being fractured using a razor blade (PDF). This material is available free of charge via the Internet at http://pubs.acs.org.